Answers to Reviewer 1 comments

Precipitable water vapor retrievals using a ground infrared sky camera in subtropical South America

Elion Daniel Hack, Theotonio Pauliquevis, Henrique Melo Jorge Barbosa, Marcia Akemi Yamasoe, Dimitri Klebe, and Alexandre Lima Correia
Manuscript ID: amt-2022-283

We address below all comments presented by Reviewer 1 of our manuscript *"Precipitable water vapor retrievals using a ground infrared sky camera in subtropical South America"*. We thank the reviewer for their questions and suggestions. We have expanded our discussions and added clarifications to the revised manuscript as requested. We believe the modifications prompted by the reviewer helped frame our methodology in a more precise fashion.

RC1: 'Comment on amt-2022-283', Anonymous Referee #1, 25 Nov 2022

Precipitable water vapor retrievals using a ground infrared sky camera in subtropical South America by Elion Hack

This work analyzed IR imagery produced by the ASIVA sky camera to measure the downwelling radiance at 10-12 μm, L_λ. The method for retrieving the atmospheric PWV in this study used the relative distribution of humidity profile climatology of the sampling location. The results can be useful to applications seeking to study the role of spatial-temporal transformations of water vapor in the atmosphere, especially in time-sensitive processes such as the initiation of convection. In that respect the present study has a high potential for publication after the incorporation of the comments/suggestions as given below:

1. *You have used Radiosonde data for retrieving the atmospheric PWV. But the Radiosonde and sunphotometer data are also associated with errors. Explain the possible sources of Radiosonde and sunphotometer errors in your analysis.*

We thank the reviewer for this suggestion. The sources of errors associated with PWV retrievals by radiosondes and sunphotometers are indeed important since these instruments are considered benchmarks against which any new methodology needs to be compared. According to Pérez-Ramírez et al. (2014), sunphotometer results can have systematic calibration uncertainties corresponding to 4-5% of the PWV retrievals, and random radiance measurement uncertainties below 1%. Besides that, simplifications in modeling the atmospheric water vapor radiative transmission process can lead to about 5% uncertainty. Hence, a final number that has been quoted in the literature of 10% uncertainty in PWV retrievals by AERONET corresponds to a composition of all these sources of errors, which is the figure we used in this work. For radiosondes, Castro-Almazán et al. (2016) argue that calibration biases can lead to up to 5% uncertainty in the retrieved PWV. They also indicate daytime radiosonde launches can have a dry bias of 2-8% due to the solar heating of the

humidity sensor. Following the results from a semi-empirical analysis by Castro-Almazán et al. (2016) we use in this work a figure of 3% uncertainty for radiosonde PWV retrievals. We have addressed this issue by adding the following text to the revised manuscript, lines 115-135:

"An Aerosol Robotic Network (AERONET) sunphotometer (Holben et al., 1998), colocated with the ASIVA sky imager (23.56° S, 46.74° W, 786 m asl), was used to independently assess columnar PWV retrievals. The sunphotometer is equipped with a collimated photodetector, that measures solar and sky radiance at different wavelengths. The integrated PWV content is determined from the attenuation of solar radiation at 940 nm along its optical path in the atmosphere by applying a modified Beer-Lambert-Bouguer law (Pérez-Ramírez et al., 2014). Only level 2.0 calibrated PWV data from AERONET (Smirnov et al., 2000) were used in this work. According to Pérez-Ramírez et al. (2014), sunphotometer results can have systematic calibration uncertainties corresponding to 4-5% of the PWV retrievals, and random radiance measurement uncertainties below 1%. Besides that, simplifications in modeling the atmospheric water vapor radiative transmission process can lead to about a 5% PWV uncertainty. Hence, a final number that has been quoted in the literature of 10% uncertainty in PWV retrievals by AERONET corresponds to a composition of all these sources of errors, which is the figure used in this work.

AERONET PWV retrievals have been performed in Sao Paulo from November 2000 to the present day, with some gaps from February 2012 to November 2014. We used the AERONET retrievals in two different ways in this work. First, all available PWV retrievals were used in comparison with radiosonde data. This was done by averaging sunphotometer retrievals within ±30 min of each 12:00 UTC (09:00 LT) sounding launch. Secondly, AERONET PWV retrievals were compared to ASIVA estimates for selected days of clear sky, or with few clouds, on which both time series were measured.

2.3 Vertical water vapor profiles and integrated PWV

Radiosondes have been regularly launched from the Campo de Marte airfield (International Civil Aviation Organization code SBMT, latitude: 23.52◦ S, longitude: 46.63◦ W, altitude: 722 m asl) at 0:00 and 12:00 UTC (21:00 and 09:00 LT, respectively). The airfield is 11 km distant, and 64 m below in altitude, from the ASIVA and sunphotometer operation site. Direct measurements of the specific humidity along the vertical radiosonde profile are integrated to yield the PWV for each radiosonde launch. Castro-Almazán et al. (2016) argue that calibration biases can lead to up to 5% uncertainty in the retrieved PWV by radiosondes. They also indicate daytime radiosonde launches can have a dry bias of 2-8% due to the solar heating of the humidity sensor. Following the results from a semi-empirical analysis by Castro-Almazán et al. (2016) we use in this work a figure of 3% uncertainty for radiosonde PWV retrievals. All radiosonde data was accessed via the University of Wyoming website (https://weather.uwyo.edu/upperair/sounding.html, accessed 19 August 2022 12:00 UTC).

Radiosonde data were used in this work in multiple ways that will be discussed in greater detail further ahead. Firstly, when available, a radiosonde vertical profile at 09:00 LT is used to derive one type of LUT where L_λ is simulated for a range of PWV. This is done by normalizing the given radiosonde profile to match each PWV in the simulated range."

2. *How were these thresholds determined to identify clear or partially cloudy pixels? You should include some explanation of these values.*

We thank the reviewer for this crucial question. The rationale for our methodology is based on the assumption the acquired imagery corresponds to clear or partially clear skies. It cannot be directly applied to completely overcast sky conditions. Because clear sky pixels correspond to significantly lower spectral radiance (L_λ) emissions compared to clouds, and since there can be many pixels in the detector array (644 x 512) for a given airmass, it is often possible to determine a minimum L_λ envelope as a function of airmass that corresponds to clear sky pixels. We have modified Fig. 1b (below) to help explain how cloudy and partially cloudy pixels were identified and removed from the analyses. This was done by excluding pixels with either (a) high spatial L_λ variability, or (b) above a maximum L_λ threshold. The spatial variability filter was applied by computing, for a given pixel, the L_λ sample standard deviation for the 8 nearest neighboring pixels, and removing cases with standard deviation above 0.07 W m^{-2} μm^{-1} sr^{-1}. These correspond to the data points identified as "Filter A" in Fig. 1b. The maximum L_λ threshold filter depends on the pixel airmass, the instrument temperature, and the cloud type possibly present (e.g. it can be more complex to exclude very cold thin cirrus clouds). This limit is defined, for a given temperature condition, as the median L_λ computed at airmass 3.00±0.01. In the particular example shown in Fig. 1b, this threshold was 3.0 W m^{-2} μm^{-1} sr^{-1}, as indicated by the horizontal dashed line. Data points identified as "Filter B" in Fig. 1b were eliminated by the threshold filter. Finally, after applying filters (a) and (b), the minimum L_λ envelope is defined as the median of L_λ, calculated for each ±0.001 airmass interval around discrete airmass values in the LUTs, for airmasses below 2.0. These correspond to "Median envelope" data points in Fig. 1b. Besides clouds, this procedure also excludes pixels corresponding to physical structures in the vicinity of the detector.

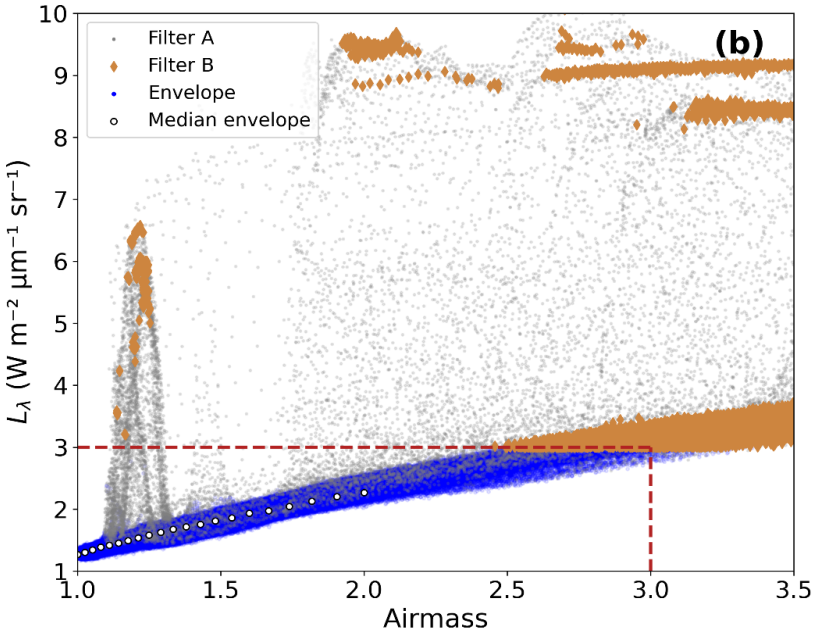

Figure 1b. Spectral radiance (L_λ) measured at ASIVA's channel 4 (10-12 μm) on 2017-07-06 at 15:17 UTC (12:17 LT) in Sao Paulo as a function of the airmass. Cloudy and physical structure pixels were eliminated by applying the procedure described in the text (Filters A and B). Envelope data points correspond to clear sky L_λ, from which medians were computed at specific airmass values.

This explanation was added to the revised manuscript text, originally in lines 97-109:

> "The spectral radiance can then be analyzed as a function of the observation geometry. In this work, we study the spectral radiance as a function of airmass, defined as $1/\cos(\theta)$, where θ is the view zenith angle for each pixel. Figure 1 shows, as an example, L_λ measurements using ASIVA's infrared channel 4. Figure 1a presents L_λ for each image pixel ~~of the image~~, and Fig. 1b shows L_λ as a function of airmass. The lower L_λ envelope in Fig. 1b, clearly defined, corresponds to the emission of cooler regions observed in the image, which are those of clear sky, while the points with greater radiance are warmer bodies such as clouds and nearby structures in the camera's view. It is expected that near the zenith the measured radiance for clear skies will be lower than in regions closer to the horizon. This is clearly observable in Fig. 1a, and in the shape of the lower envelope in Fig. 1b. This is due to the thinner atmosphere between the camera and outer space at the zenith, with this thickness increasing with the airmass. Cloudy and partially cloudy pixels were identified and removed from the analyses by excluding pixels with either (a) high spatial L_λ variability, or (b) above a maximum L_λ threshold. The spatial variability filter was applied by computing, for a given pixel, the L_λ sample standard deviation for the 8 nearest neighboring pixels, and removing cases with standard deviation above 0.07 W m^{-2} μm^{-1} sr^{-1}. ("Filter A" data points in Fig. 1b). The maximum L_λ threshold filter depends on the pixel airmass, the instrument temperature, and the cloud type possibly present (e.g. it can be more complex to exclude very cold thin cirrus clouds). This limit is defined, for a given temperature condition, as the median L_λ computed at airmass 3.00±0.01. In the particular example shown in Fig. 1b, this threshold was 3.0 W m^{-2} μm^{-1} sr^{-1}, as indicated by the horizontal dashed line. Data points identified as "Filter B" in Fig. 1b were eliminated by the threshold filter. Finally, after applying filters (a) and (b), the minimum L_λ envelope is defined as the median of L_λ, calculated for each ±0.001 airmass interval, around discrete airmass values in the LUTs described further ahead, for airmasses below 2.0. These correspond to "Median envelope" data points in Fig. 1b. At the channel 4 range, the sky radiance L_λ strongly depends on the amount of columnar PWV, its vertical distribution and temperature, the optical path from the emission to the sensor, and the transmittance of the medium. Using radiative transfer simulation software, such as libRadtran, the expected L_λ as a function of airmass can be calculated for a series of atmospheric humidity profiles. A PWV retrieval can be obtained by determining, for a given humidity profile, which of the simulations most closely matches the measured lower envelope such as the one shown in Fig 1b."

3. *There are three questions, which might be interesting for the readers if you could answer them in the conclusions:*
   i) Overall, do you consider the quality of the Precipitable water vapor retrievals using a ground infrared sky camera to be "good" or "satisfying"? Is the quality good enough to provide benefits for users as well as a repository of data?
   ii) Could the Precipitable water vapor possibly be improved in future work?
   iii) How does the quality of Precipitable water vapor retrievals using a ground infrared sky camera compare to earlier studies? How do the validation results of this study compare to earlier work?

We thank the reviewer for identifying these issues. In part, some of these questions were addressed in the Discussion section. As requested, we have added more details in the Conclusion section of the revised manuscript. To discuss the questions raised by the reviewer specifically, (i) for the cases analyzed in the work, the sky camera PWV retrievals show biases within a few millimeters w.r.t. radiosonde or sunphotometer retrievals (cf. Table 2 added in the revised manuscript, included below for convenience). Certainly, more statistics are necessary to study the reliability and usefulness of the technique described in this initial work, so a data repository can be established in the future. One benefit users could get only with this type of instrumentation is the azimuthal distribution of PWV or the PWV sky mapping. This initial result shown in this work cannot be derived from other current techniques, although it will require further investigation to assess its accuracy. Regarding (ii), one possible way to improve the retrievals would be to operate the ASIVA instrument alongside radiosonde launches with a higher temporal frequency, to better frame daily variations in atmospheric profiles. Another possibility is to use other radiometric channels in the instrument to explore or study differential water vapor transmittance for different wavelengths, which could return extra information on the vertical water vapor profile. On the subject of validation efforts (iii), that is a crucial aspect of any new technique. This will require extensive testing under different environmental conditions and site locations. In this work, we show the ASIVA methodology development and initial comparisons with established techniques based on radiosonde and sunphotometer PWV retrievals. Such comparisons show daily PWV averages and standard deviations agree within a few millimeters (cf. Table 2), but also that there is a coherence of temporal trends during the day, i.e. increasing or decreasing PWV in time series of both ASIVA and AERONET retrievals (cf. Figs 7 and 8). We have added Table 2 to the revised manuscript, where we compare our PWV results to the established techniques using radiosondes and AERONET, and the corresponding discussion, at line 347:

> "The largest PWV discrepancy between the two series at ~16:00 UTC is about the same size as the differences discussed in Fig. 8b. The ASIVA PWV around 12:00 UTC is compatible with the radiosonde data point within the 3% uncertainty range. The retrieved ASIVA PWV time series in Fig. 8b is very similar to the solution using the medium altitude synthetic profile (green curve in Fig. 7c). The conclusion here is that there are inherent discrepancies between the source radiosonde data and the AERONET PWV retrieval for this particular complex case. Hence the radiosonde-derived ASIVA series will also show differences from the AERONET results. Such differences, however, are still under the variations that can be expected statistically. The ASIVA retrieval results discussed in Fig. 8, based on radiosonde profile data, correspond to the solution circled "4" in Fig. 3b.
>
> Table 2 shows a summary of PWV statistics for ASIVA, sunphotometer, and radiosonde retrievals, for the cases analyzed in Figs. 7 and 8. Although the PWV can vary along the day, Table 2 shows the daytime number of samples, average, and sample standard deviation for the three instruments, for the sake of comparison. The ASIVA can operate at a higher frequency than AERONET, as exemplified in Figs. 7d and 8d, with 152 daytime retrievals. The PWV sample standard deviations behave similarly when comparing ASIVA and AERONET. A day with larger PWV variations (Figs. 7a and 8a) shows the AERONET standard deviation of 1.4 mm, while the ASIVA retrieval strategies varied between 1.1 and 1.7 mm. When smaller PWV variations were observed (Figs. 7d and 8d), the AERONET standard deviation was 0.5 mm while ASIVA showed 0.4 to 0.7 mm. Differences between the daytime average PWV retrieved by ASIVA and either AERONET or radiosondes are generally within a few millimeters. In particular, for the cases under analysis the ASIVA retrieval method using the radiosonde

humidity profile discussed in Fig. 8 (RS F8 in Table 2) showed smaller absolute biases w.r.t. the radiosonde PWV, ranging from -2.1 to +0.9 mm, than the AERONET biases, which varied from -3.7 to -0.2 mm. However, since only the single available daytime radiosonde profile was used in Fig. 8 ASIVA retrievals, this result is contingent on the atmospheric profile remaining relatively stable throughout the day, and more statistics are necessary to study these results in greater detail."

Table 2. ASIVA, sunphotometer, and radiosonde PWV retrieval statistics for the cases shown in Figs. 7 and 8.

Figs. 7/8		a	b	c	d
Date		2018-02-07	2018-02-09	2018-08-19	2017-07-06
Number of daytime measurements					
ASIVA		36	18	20	152
Sunphotometer (SP)		38	32	38	36
Radiosonde (RS)		1	1	1	1
Average daytime PWV (sample standard deviation), in mm					
ASIVA	SH F7	23.4 (1.7)	26.2 (1.1)	19.7 (1.2)	14.0 (0.7)
	SM F7	20.6 (1.5)	23.0 (1.0)	17.4 (1.0)	12.4 (0.6)
	SL F7	15.8 (1.1)	17.6 (0.7)	13.4 (0.8)	9.6 (0.4)
	RS F8	19.9 (1.2)	27.2 (1.1)	17.2 (0.9)	12.4 (0.6)
SP		19.4 (1.4)	23.5 (1.0)	14.4 (0.6)	12.5 (0.5)
RS		21.9	27.2	16.3	12.7
Average bias: Instrument PWV - Reference PWV, in mm					
ASIVA - SP	SH F7	4.0	2.6	5.3	1.4
	SM F7	1.3	-0.5	3.0	-0.1
	SL F7	-3.6	-5.9	-1.0	-2.9
	RS F8	0.5	3.7	2.8	-0.1
ASIVA - RS	SH F7	1.4	-1.1	3.4	1.2
	SM F7	-1.3	-4.2	1.1	-0.3
	SL F7	-6.2	-9.7	-2.9	-3.1
	RS F8	-2.1	0.0	0.9	-0.4
SP - RS		-2.6	-3.7	-1.9	-0.2

SH F7, SM F7, SL F7 refer to the ASIVA retrievals in Fig. 7 using the synthetic high, medium, and low altitude profiles, respectively. RS F8 is the ASIVA retrieval using the radiosonde profile in Fig. 8.

Besides the text in the Discussion section, we have added more information to the Conclusions, lines 401-415, in the revised manuscript:

"From our analyses, we showed that a key factor is the relative vertical distribution of water vapor, i.e., how close to the surface the bulk of the water vapor radiative emission occurs. If such a typical relative distribution of water vapor is known a priori from the climatology of the sampling location, the method discussed here can be used to derive the PWV. If complementary radiosonde profiles are available, the proposed method can retrieve PWV time series that in general show adequate agreement with independent AERONET retrievals and can also generate PWV maps that are not possible with other current techniques. In one

study case, under very stable atmospheric conditions, we showed the precision of consecutive retrievals to be about 1.9%, with an average PWV of 12.01 mm about 2.8% below the AERONET estimate. For comparison, radiosondes at the sampling site in Sao Paulo have shown (Fig. 4) a positive bias towards AERONET retrievals corresponding to about 6.3% (0.75 mm), and an RMS deviation of 15.8% (1.9 mm), both considering a reference PWV of 12.0 mm. Daytime ASIVA PWV averages and standard deviations are compatible with AERONET and radiosonde retrievals within a few millimeters (Table 2). Full validation of the technique will require extensive testing under a variety of environmental conditions and site locations to ascertain its usefulness and reliability.

The method can be applied at any time of the day, with a repeatability of a few minutes, and under partially cloudy conditions. We hypothesize that by using sky imagery acquired at other IR wavelengths it can be possible to simultaneously retrieve the PWV and the vertical distribution of humidity in the atmosphere, independently from ancillary instrumentation. These results can be useful to applications seeking to study the role of spatial-temporal transformations of water vapor in the atmosphere, especially in time-sensitive processes such as the initiation of convection."

Answers to Reviewer 2 comments

Precipitable water vapor retrievals using a ground infrared sky camera in subtropical South America

Elion Daniel Hack, Theotonio Pauliquevis, Henrique Melo Jorge Barbosa, Marcia Akemi Yamasoe, Dimitri Klebe, and Alexandre Lima Correia
Manuscript ID: amt-2022-283

We address below the comments by Reviewer 2 about our manuscript *"Precipitable water vapor retrievals using a ground infrared sky camera in subtropical South America"*. We thank the reviewer for these comments and suggestions. As requested, we have included further discussions in the revised manuscript. These modifications contributed to clarifying key aspects of our methodology and framing the text more precisely.

RC2: 'Comment on amt-2022-283', Anonymous Referee #2, 19 Dec 2022

Review on Precipitable water vapor retrievals using a ground infrared sky camera in subtropical South America.

The paper addresses an important scientific question, as water vapor, an important trace gas, is known to be difficult to represent spatially and temporally with current instrumentation and this instrumentation could help in this regard. The idea of the paper is novel, taking from Mims et al. (2011) idea of using an IR thermometer to point to the sky, but improving it with a camera that can give us spatial distribution information. The conclusions could be extended a bit (see my comment below), and I cannot say they are substantial but they are a first approximation to the problem of retrieving water vapor information with a ground infrared sky camera. The methods are clearly outlined and, in my opinion, the assumptions are valid. The results are just a start (one site, some periods of a few days, ...), but I think they are enough for a first approximation to the topic and determining the best approach for extended studies. Regarding the description of the experiments, I think that some things are missing but in general the description is good (see my specific comments below). Title, abstract, and bibliography are correct in my opinion, and the presentation is well structured and clear. The language is generally correct in my opinion (see technical issues for some small corrections). I therefore recommend minor changes in the paper before it is ready for publication.

Specific comments
It is not clear how the synthetic profiles are obtained. It would be interesting also to indicate the equations of these profiles.

We thank the reviewer for this comment. The synthetic profiles are discussed in manuscript Section 2.4. They were obtained from wintertime radiosonde profiles with clear skies or few clouds. Within this subset, we aggregated cases for which the median humidity altitude was either “low altitude” or “high altitude”. The synthetic profiles were built by visual inspection, representing simplified versions of these two classes of vertical humidity distribution. They do not refer to the total amount of integrated humidity (i.e. the PWV), but rather to the relative vertical distribution of humidity, which is crucial for describing the measured downwelling infrared radiance L_λ. The simplified profiles capture this essential information used in the retrieval process. We included in the revised manuscript a table with the data points representing each of the profiles, and adapted the paragraph starting at line 157:

> “The variability of the vertical profile of water vapor was studied on winter days with clear skies or few clouds. Winter was used because it is the season with the majority of available measurements since it is drier and therefore with less frequent clouds than summer. A dataset with 09:00 LT radiosondes for the austral winter months (July-September) was scrutinized to select profiles that represented fewer cloud cover conditions. This was done by taking the frequency of AERONET PWV retrievals within ±30 min from the radiosonde launching time as a proxy for the occurrence of clouds. Radiosonde profiles were retained for analysis whenever at least 5 sunphotometer retrievals were successful within the 1 h time matching window. The median humidity altitude in the radiosonde subset was investigated to identify typical “low altitude” and “high altitude” profiles, regardless of their absolute PWV, and average profiles were computed (Fig. 2). From these, synthetic simplified versions of such profiles were built by visual inspection. A~~n average~~ profile corresponding to “medium altitude” was computed as the average between the low and high altitude profiles. Figure 2 shows the three resulting synthetic profiles, which are meant to be used when no radiosonde information is available for a given day, as described further below. Table 1 shows the data points used in the profiles. The same synthetic profiles were used for summer PWV retrievals, i.e. by keeping the same relative vertical distribution of water vapor, while the method retrieves PWV values within the expected range for summer. Even though there will always be discrepancies between real radiosondes and synthetic profiles, in general such differences show little influence on the final integrated PWV.”

Table 1. Synthetic atmospheric humidity profiles shown in Fig. 2.

	Low altitude	Medium altitude	High altitude
Atmospheric pressure (hPa)	Water vapor mixing ratio (g kg^{-1})		
930	7.000	7.750	8.500
870	6.000	6.875	7.667
810	0.300	6.000	6.833
755	0.273	0.900	6.069
750	0.271	0.891	6.000
700	0.246	0.797	1.500
300	0.050	0.050	0.050

L178-179. It is claimed that averaged profiles are also used but then in lines 185-189 this is not mentioned.

We thank the reviewer for this observation. This refers to section "2.5 Radiative transfer simulations" in the manuscript. This section describes the multiple ways the libRadtran package was used in the work. The software can be used with internal atmospheric profiles (i.e. mid-latitude summer, tropical, etc.), or with user-provided profiles. In the initial step of the work, we studied how the vertical distribution of humidity affects the measured L_λ. We compared libRadtran L_λ simulations using its internal profiles, average humidity profiles, and profiles from single radiosonde launches, all normalized to the same PWV. The results of this comparison were analyzed in Fig. 5. In a later step of the work we developed look-up tables of measured vs. simulated L_λ, that allow retrieving PWV estimates under different methodological strategies. For the libRadtran L_λ simulations in these look-up tables, we have used synthetic and radiosonde humidity profiles. Therefore there is no inconsistency in the passage noted by the reviewer: lines 178-179 describe average profiles used with libRadtran in the first part of the work, while lines 185-189 describe the libRadtran profiles used later. We have changed the text in lines 172-182 in the revised manuscript to seek a better distinction between these cases:

> "In this work, we used the libRadtran software package, a library for atmospheric radiative transfer calculations (Mayer and Kylling, 2005; Emde et al., 2016). The program solves the radiative transfer equation for a given atmospheric setup and then obtains simulated radiances and irradiances for a specified viewing geometry. We used the DISORT (discrete ordinates) method to solve the radiative transfer equation and the plane-parallel atmosphere approximation. Internal and user-provided atmospheric humidity profiles were used in different steps of the work. Three internal standard atmospheric profiles were studied ~~in this work~~: tropical, mid-latitude summer, and mid-latitude winter (Anderson et al., 1986), seeking to understand how they might represent the physical conditions at the observing site. Even though the site location is in the subtropics, midlatitude profiles were included in the analyses for the sake of comparison. We also used ~~alternative~~ average seasonal atmospheric profiles as input, ~~representing seasonal averages~~ obtained from radiosonde data from 2005 to 2015, to study the influence of the vertical distribution of humidity on simulated L_λ.
> Two types of LUTs were computed with libRadtran in this study. Firstly, when radiosonde data is not available, a LUT of simulated $L^{c,s}_{\lambda,i}$ as a function of airmass was produced for the high, medium, and low altitude synthetic humidity profiles (presented in Sect. 2.4)"

L196-197. It is claimed that cloudy pixels are removed, but it is not stated how (by visual inspection, with a threshold value in L, ...).

We thank the reviewer for this very important question, which was also identified by another reviewer. Therefore we repeat the explanation given elsewhere. We have modified Fig. 1b (below) to help explain how cloudy and partially cloudy pixels were identified and removed from the analyses. This was done by excluding pixels with either (a) high spatial L_λ variability,

or (b) above a maximum L_λ threshold. The spatial variability filter was applied by computing, for a given pixel, the L_λ sample standard deviation for the 8 nearest neighboring pixels, and removing cases with standard deviation above 0.07 W m^{-2} μm^{-1} sr^{-1}. These correspond to the data points identified as "Filter A" in Fig. 1b. The maximum L_λ threshold filter depends on the pixel airmass, the instrument temperature, and the cloud type possibly present (e.g. it can be more complex to exclude very cold thin cirrus clouds). This limit is defined, for a given temperature condition, as the median L_λ computed at airmass 3.00±0.01. In the particular example shown in Fig. 1b, this threshold was 3.0 W m^{-2} μm^{-1} sr^{-1}, as indicated by the horizontal dashed line. Data points identified as "Filter B" in Fig. 1b were eliminated by the threshold filter. Finally, after applying filters (a) and (b), the minimum L_λ envelope is defined as the median of L_λ, calculated for each ±0.001 airmass interval around discrete airmass values in the LUTs, for airmasses below 2.0. These correspond to "Median envelope" data points in Fig. 1b. Besides clouds, this procedure also excludes pixels corresponding to physical structures in the vicinity of the detector.

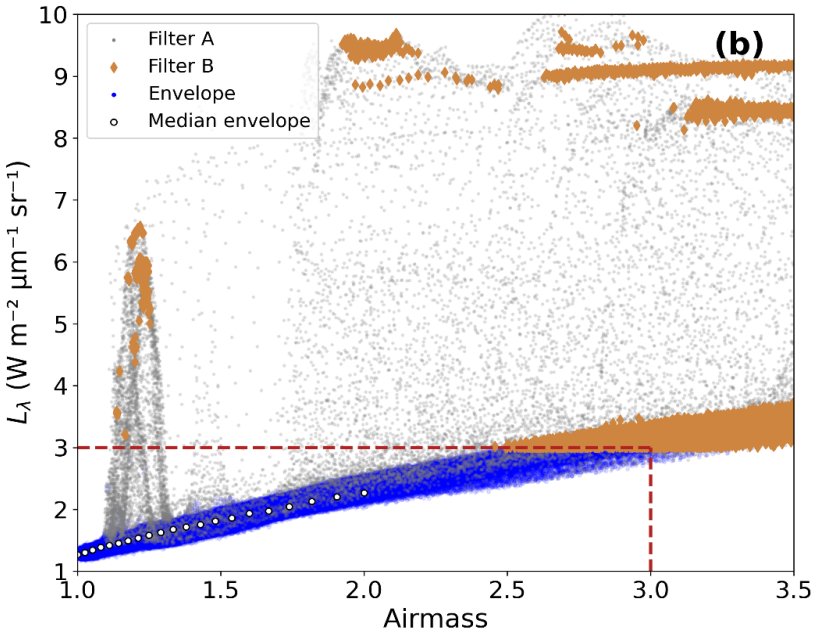

Figure 1b. Spectral radiance (L_λ) measured at ASIVA's channel 4 (10-12 μm) on 2017-07-06 at 15:17 UTC (12:17 LT) in Sao Paulo as a function of the airmass. Cloudy and physical structure pixels were eliminated by applying the procedure described in the text (Filters A and B). Envelope data points correspond to clear sky L_λ, from which medians were computed at specific airmass values.

This explanation was added to the revised manuscript text, originally in lines 97-109:

"The spectral radiance can then be analyzed as a function of the observation geometry. In this work, we study the spectral radiance as a function of airmass, defined as 1/cos(θ), where θ is the view zenith angle for each pixel. Figure 1 shows, as an example, L_λ measurements using ASIVA's infrared channel 4. Figure 1a presents L_λ for each image pixel ~~of the image~~, and Fig. 1b shows L_λ as a function of airmass. The lower L_λ envelope in Fig. 1b, clearly defined, corresponds to the emission of cooler regions observed in the image, which are those of clear sky, while the points with greater radiance are warmer bodies such as clouds and nearby structures in the camera's view. It is expected that near the zenith the measured radiance for

clear skies will be lower than in regions closer to the horizon. This is clearly observable in Fig. 1a, and in the shape of the lower envelope in Fig. 1b. This is due to the thinner atmosphere between the camera and outer space at the zenith, with this thickness increasing with the airmass. Cloudy and partially cloudy pixels were identified and removed from the analyses by excluding pixels with either (a) high spatial L_λ variability, or (b) above a maximum L_λ threshold. The spatial variability filter was applied by computing, for a given pixel, the L_λ sample standard deviation for the 8 nearest neighboring pixels, and removing cases with standard deviation above 0.07 W m^{-2} μm^{-1} sr^{-1}. ("Filter A" data points in Fig. 1b). The maximum L_λ threshold filter depends on the pixel airmass, the instrument temperature, and the cloud type possibly present (e.g. it can be more complex to exclude very cold thin cirrus clouds). This limit is defined, for a given temperature condition, as the median L_λ computed at airmass 3.00±0.01. In the particular example shown in Fig. 1b, this threshold was 3.0 W m^{-2} μm^{-1} sr^{-1}, as indicated by the horizontal dashed line. Data points identified as "Filter B" in Fig. 1b were eliminated by the threshold filter. Finally, after applying filters (a) and (b), the minimum L_λ envelope is defined as the median of L_λ, calculated for each ±0.001 airmass interval, around discrete airmass values in the LUTs described further ahead, for airmasses below 2.0. These correspond to "Median envelope" data points in Fig. 1b. At the channel 4 range, the sky radiance L_λ strongly depends on the amount of columnar PWV, its vertical distribution and temperature, the optical path from the emission to the sensor, and the transmittance of the medium. Using radiative transfer simulation software, such as libRadtran, the expected L_λ as a function of airmass can be calculated for a series of atmospheric humidity profiles. A PWV retrieval can be obtained by determining, for a given humidity profile, which of the simulations most closely matches the measured lower envelope such as the one shown in Fig 1b."

In general, I am missing some table showing the statistics in the different methodologies/situations to compare them to each other easily. The conclusions could also benefit from this kind of information.

We thank the reviewer for this important suggestion. We have added a table to the revised manuscript, comparing our PWV results to the established techniques using radiosondes and AERONET, and the corresponding discussion, at line 347:

"The largest PWV discrepancy between the two series at ~16:00 UTC is about the same size as the differences discussed in Fig. 8b. The ASIVA PWV around 12:00 UTC is compatible with the radiosonde data point within the 3% uncertainty range. The retrieved ASIVA PWV time series in Fig. 8b is very similar to the solution using the medium altitude synthetic profile (green curve in Fig. 7c). The conclusion here is that there are inherent discrepancies between the source radiosonde data and the AERONET PWV retrieval for this particular complex case. Hence the radiosonde-derived ASIVA series will also show differences from the AERONET results. Such differences, however, are still under the variations that can be expected statistically. The ASIVA retrieval results discussed in Fig. 8, based on radiosonde profile data, correspond to the solution circled "4" in Fig. 3b.

Table 2. ASIVA, sunphotometer, and radiosonde PWV retrieval statistics for the cases shown in Figs. 7 and 8.

Figs. 7/8		a	b	c	d
Date		2018-02-07	2018-02-09	2018-08-19	2017-07-06
Number of daytime measurements					
ASIVA		36	18	20	152
Sunphotometer (SP)		38	32	38	36
Radiosonde (RS)		1	1	1	1
Average daytime PWV (sample standard deviation), in mm					
ASIVA	SH F7	23.4 (1.7)	26.2 (1.1)	19.7 (1.2)	14.0 (0.7)
	SM F7	20.6 (1.5)	23.0 (1.0)	17.4 (1.0)	12.4 (0.6)
	SL F7	15.8 (1.1)	17.6 (0.7)	13.4 (0.8)	9.6 (0.4)
	RS F8	19.9 (1.2)	27.2 (1.1)	17.2 (0.9)	12.4 (0.6)
SP		19.4 (1.4)	23.5 (1.0)	14.4 (0.6)	12.5 (0.5)
RS		21.9	27.2	16.3	12.7
Average bias: Instrument PWV - Reference PWV, in mm					
ASIVA - SP	SH F7	4.0	2.6	5.3	1.4
	SM F7	1.3	-0.5	3.0	-0.1
	SL F7	-3.6	-5.9	-1.0	-2.9
	RS F8	0.5	3.7	2.8	-0.1
ASIVA - RS	SH F7	1.4	-1.1	3.4	1.2
	SM F7	-1.3	-4.2	1.1	-0.3
	SL F7	-6.2	-9.7	-2.9	-3.1
	RS F8	-2.1	0.0	0.9	-0.4
SP - RS		-2.6	-3.7	-1.9	-0.2

SH F7, SM F7, SL F7 refer to the ASIVA retrievals in Fig. 7 using the synthetic high, medium, and low altitude profiles, respectively. RS F8 is the ASIVA retrieval using the radiosonde profile in Fig. 8.

Table 2 shows a summary of PWV statistics for ASIVA, sunphotometer, and radiosonde retrievals, for the cases analyzed in Figs. 7 and 8. Although the PWV can vary along the day, Table 2 shows the daytime number of samples, average, and sample standard deviation for the three instruments, for the sake of comparison. The ASIVA can operate at a higher frequency than AERONET, as exemplified in Figs. 7d and 8d, with 152 daytime retrievals. The PWV sample standard deviations behave similarly when comparing ASIVA and AERONET. A day with larger PWV variations (Figs. 7a and 8a) shows the AERONET standard deviation of 1.4 mm, while the ASIVA retrieval strategies varied between 1.1 and 1.7 mm. When smaller PWV variations were observed (Figs. 7d and 8d), the AERONET standard deviation was 0.5 mm while ASIVA showed 0.4 to 0.7 mm. Differences between the daytime average PWV retrieved by ASIVA and either AERONET or radiosondes are generally within a few millimeters. In particular, for the cases under analysis the ASIVA retrieval method using the radiosonde humidity profile discussed in Fig. 8 (RS F8 in Table 2) showed smaller absolute biases w.r.t. the radiosonde PWV, ranging from -2.1 to +0.9 mm, than the AERONET biases, which varied from -3.7 to -0.2 mm. However, since only the single available daytime radiosonde profile was used in Fig. 8 ASIVA retrievals, this result is contingent on the atmospheric profile remaining

relatively stable throughout the day, and more statistics are necessary to study these results in greater detail."

The flowchart in Figure 3 looks very clear to me, so I congratulate the authors for it.

We thank the reviewer for this observation. Indeed we have dedicated an appreciable amount of time to developing the flowchart in Fig. 3 to convey all key aspects of the methodology discussed in the manuscript. We appreciate the mention.

Technical issues
1. L.155 measured --> compared

As requested, the sentence was changed to reflect the fact data from AERONET and ASIVA were compared, such as:

"AERONET PWV retrievals have been performed in Sao Paulo from November 2000 to the present day, with some gaps from February 2012 to November 2014. We used the AERONET retrievals in two different ways in this work. First, all available PWV retrievals were used in comparison with radiosonde data. This was done by averaging sunphotometer retrievals within ± 30 min of each 12:00 UTC (09:00 LT) sounding launch. Secondly, AERONET and ASIVA PWV retrievals were compared ~~to ASIVA estimates for~~ on selected days ~~of~~ with clear sky~~,~~ or ~~with~~ few clouds~~, on which both time series were measured~~."

2. L.158. I am not sure this is completely correct, there can be places in which winter is dry and with clouds. It also depends on what "dry" really means (less relative humidity? less specific humidity?).

We agree with the points raised by the reviewer. Specifically, the sentence relates to the weather conditions observed in our sampling site. Other sites can have different typical wintertime conditions. In our case, the word "drier" refers to lower yearly PWV values observed at this time of the year. The text in lines 157-160 has been adapted in the revised manuscript to clarify these points, such as:

"The variability of the vertical profile of water vapor was studied on winter days with clear skies or few clouds. Winter was used because it is the season with the majority of available measurements since in Sao Paulo it is drier (i.e. lowest yearly PWV observed) and therefore with less frequent clouds than summer. A dataset with 09:00 LT radiosondes for the austral winter months (July-September) was scrutinized to select profiles that represented fewer cloud cover conditions."

3. L296-298. Maybe rewrite the sentence as: "Thus, provided that both the temporal trend and variability from the two series can be equivalent,...".

We thank the reviewer for this suggestion. The revised manuscript was updated to reflect this change:

> "If the ASIVA retrievals were to match AERONET, we would need to use a synthetic profile with a slightly more elevated median for the humidity distribution than the one in the medium altitude profile (cf. Fig. 2). Thus, provided that both the temporal trend and variability from the two series can be considered equivalent ~~in both series~~, the PWV distance between them can be seen as a proxy for the effective median humidity distribution along the vertical."